Function and regulation of chloroplast peroxiredoxin IIE

Anna Dreyer[1$], Patrick Treffon[1$§], Daniel Basiry[1], Anna Maria Jozefowicz[2], Andrea Matros[2#], Hans-Peter Mock[2], Karl-Josef Dietz[1*]

[1] Department of Biochemistry and Physiology of Plants, Faculty of Biology, University of Bielefeld, 33615 Bielefeld, Germany; ptreffon@umass.edu (PT); anna.dreyer@uni-bielefeld.de (AD); danielbasiry@gmx.de (DB)

[2] Applied Biochemistry Group, Leibniz Institute for Plant Genetics and Crop Plant Research (IPK), 06466 Seeland, OT Gatersleben, Germany; jozefowicz@ipk-gatersleben.de (AMJ); andrea.matros@icloud.com (AM); mock@ipk-gatersleben.de (HPM)

[$] shared first authorship due to equal contribution to this research

[§] current affiliation PT: Department of Biochemistry and Molecular Biology, University of Massachusetts Amherst, USA

[#] current affiliation AM: Australian Research Council Centre of Excellence in Plant Cell Walls, University of Adelaide, SA 5064 Adelaide, Australia

* Correspondence: karl-josef.dietz@uni-bielefeld.de; Tel. +49-521-106-5589 (KJD)

Abstract: Peroxiredoxins (PRX) are thiol peroxidases which are highly conserved throughout all biological kingdoms. Increasing evidence suggests that their high reactivity toward peroxides has a function not only in antioxidant defense but in particular in redox regulation of the cell. Peroxiredoxin IIE is one of three PRX types found in plastids and has previously been linked to pathogen defense and protection from protein nitration. However, its posttranslational regulation and its function in the chloroplast protein network remained to be explored. Using recombinant protein, it was shown that the peroxidatic Cys121 is subjected to multiple posttranslational modifications, namely disulfide formation, S-nitrosation, S-glutathionylation and hyperoxidation. Slightly oxidized glutathione fostered S-glutathionylation and inhibited activity *in vitro*. Immobilized recombinant PRX-IIE allowed trapping and subsequent identification of interaction partners by mass spectrometry. Interaction with the 14-3-3 υ protein was confirmed *in vitro* and was shown to be stimulated under oxidizing conditions. Interactions did not depend on phosphorylation as revealed by testing phospho-mimicry variants of PRX-IIE. Based on these data it is proposed that 14-3-3υ guides PRX-IIE to certain target proteins, possibly for redox regulation. These findings together with the other identified potential interaction partners of type II PRXs localized to plastids, mitochondria and cytosol provide a new perspective on the redox regulatory network of the cell.

Keywords: Peroxiredoxin, AT3G52960, glutathione, S-glutathionylation, glutaredoxin, 14-3-3 protein, phosphorylation, posttranslational modification, redox regulatory network

1. Introduction

Chloroplasts of cormophytes contain three types of peroxiredoxins (PRXs), namely classical 2-cysteine peroxiredoxin (2-CysPRX), a bacteroferritin-comigratory protein homologue PRX-Q and a type II peroxiredoxin named PRX-IIE [1,2]. The basic PRX complement of plastids is subjected to variation by the presence of isoforms, e.g., 2-CysPRX-A and -B in *Arabidopsis thaliana* (At3g11630, At5g06290), and PRX-IIE-1 and PRX-IIE-2 in *Oryza sativa* (Os06g42000, Os02g09940) [3].

PRXs are thiol peroxidases. They possess a peroxidatic cysteinyl thiol (Cys_P) with a very low pK value, and thus expose the deprotonated thiolate anion in a conserved catalytic environment. Because of this particular feature, PRXs function as highly affine and efficient thiol peroxidases [4]. The catalytic activity of 2-CysPRX, PRX-Q and type II PRX relies on a conserved second cysteine, which

49 acts as resolving thiol (Cys$_R$). Upon reaction with the peroxide substrate, the Cys$_P$-thiol forms a
50 sulfenic acid derivative which immediately is attacked by the Cys$_R$. A disulfide bond is formed
51 between Cys$_P$ and Cys$_R$. Prior to the next catalytic cycle, the disulfide bond needs to be reduced to
52 dithiols by electron donors like thioredoxin (TRX) or glutathione/glutaredoxin (GRX). The different
53 PRX forms show variation in their primary sequence, as well as the presence and position of Cys$_R$
54 and the regeneration mechanism [2].

55 The best understood plant PRX is the 2-CysPRX, which has been scrutinized with respect to its
56 catalytic properties, redox-dependent conformational dynamics, regeneration by electron
57 transmitters such as TRX and GRX/GSH and its role in the redox regulatory network of the
58 chloroplast [5–8]. In contrast PRX-Q and PRX-IIE have been studied for their peroxidatic property,
59 regeneration mechanism and their function in mutant plants with decreased protein amounts [9,10].
60 PRX-IIE belongs to the group of highly conserved atypical 2-cysteine peroxiredoxins, initially
61 discovered in the phloem of *poplar* [11]. PRX-II type PRX are found in, e.g., some but not all
62 photosynthetic cyanobacteria [12], animals/humans (PRDX5) [13] and lower and higher plants [14].

63 Previous studies showed PRXIIE to be localized in the soluble fraction of plastids. Its transcript
64 amount in *A. thaliana* leaves slightly increased in response to high light, decreased upon ascorbate
65 and NaCl treatment and remained unchanged with leaf age [1,15]. The redox titration of the dithiol-
66 disulfide transition gave a midpoint redox potential of -288 mV which is 19 and 34 mV, respectively,
67 less negative than 2-CysPRX-A and -B [1].

68 Re-reduction of the oxidized PRX-IIE from *poplar* was most efficient with GRX/glutathione
69 system, and low with glutathione and TRX [14]. The catalytic efficiency was 10^5 M^{-1}s^{-1} with tertiary
70 butylhydroperoxide (t-BOOH), fourfold less with H$_2$O$_2$, and activity was absent with cumene
71 hydroperoxide (CuOOH) [14]. Among the three GRXs (GRX-S12, -S14 and -S16) targeted to the
72 plastid in *poplar*, GRX-S12 efficiently regenerated oxidized PRX-IIE [14]. The authors suggested a
73 catalytic mechanism where the sulfenic acid derivative, formed by reaction with the peroxide
74 substrate, reacts with reduced glutathione to form a S-glutathionylated intermediate. GRX reduces
75 the Cys$_P$-SG and become itself S-glutathionylated. Another glutathione molecule then regenerates
76 GRX-SG, leading to the formation of oxidized glutathione(GSSG)[14,16].

77 This study aimed for the biochemical characterization of PRX-IIE, with focus on redox-
78 dependent posttranslational modifications of its critical cysteine residues and their impact on protein
79 function. In the light of the presumed function in redox signaling, it appeared timely to address the
80 interactome of PRX-IIE by affinity chromatography and mass-spectrometric identification. The
81 interaction with 14-3-3 υ was further validated and shown to slightly affect the peroxidase activity.
82 These novel findings point out to an additional role in redox signaling apart from its peroxidase
83 activity.

84 **2. Materials and Methods**

85 *2.1. Plant material and growth conditions*

86 *A. thaliana* Col-0 plants were grown on soil (SM Max Planck Köln, project 187509, Stender,
87 Germany) in a greenhouse with 14 h day and 10 h night at 25°C.

88 *2.2. Cloning*

89 PRX-IIE (AT3G52960), GRX-S12 (AT2G20270) and sulfiredoxin (SRX; AT1G31170) were cloned
90 into pET28a (Novagen, Darmstadt, Germany). Forward and reverse primer were designed with *NdeI*
91 and *BamHI* restriction sites, respectively (Table S1). The variants C121S, C146S, C121S/C146S, S82D,
92 T108E and T223E of PRX-IIE were generated by site-directed mutagenesis with specific primers
93 (Table *S1*). Correctness of all constructs was confirmed by DNA sequencing.

94 *2.3. Heterologous expression and purification*

95 *E. coli* BL21 (DE3)pLysS cells (Invitrogen, La Jolla, CA, USA) were transformed with plasmid
96 DNA. Overnight cultures were used to inoculate 2 L lysogeny broth medium supplemented with

97   50 µg/mL kanamycin and 20 µg/mL chloramphenicol. Protein expression was induced in the
98   exponential phase by addition of isopropyl-β-D-thiogalactopyranoside to a final concentration of
99   0.4 mM. Induced cells were grown at 37°C and 140 rpm for 4 h. Cells were harvested for 15 min at
100 5,000 xg and resuspended in lysis buffer (50 mM NaH_2PO_4, 300 mM NaCl and 10 mM imidazole,
101 pH 8.0). Cells were disrupted using lysozyme digestion followed by sonication (HF-Generator
102 GM2070 in combination with an ultrasonic converter UW2070, standard horn SH 70G and microtip
103 MS73, Bandelin, Berlin, Germany). The soluble and insoluble fractions were separated by
104 centrifugation at 20,000 xg for 45 min. His-tagged proteins were incubated with Nickel-nitrilotriacetic
105 acid (NTA) sepharose (Qiagen, Hilden, Germany) at 4°C with slight shaking for 1 h. Washing was
106 performed with washing buffer I (50 mM NaH_2PO_4, 300 mM NaCl and 20 mM imidazole, pH 8.0)
107 and subsequently washing buffer 2 (50 mM NaH_2PO_4, 300 mM NaCl, 20 (v/v) glycerol and 50 mM
108 imidazole, pH 8.0) until the OD_{280} reached zero. Elution was achieved with elution buffer (50 mM
109 NaH_2PO_4, 300 mM NaCl and 250 mM imidazole, pH 8.0). Protein containing fractions were pooled
110 and dialyzed against 40 mM K-Pi pH 7.2. After dialysis, protein concentrations were determined
111 using a molar extinction coefficient of 8480 $M^{-1} cm^{-1}$ for PRX-IIE and its variants and 9970 $M^{-1} \cdot cm^{-1}$
112 and 4470 $M^{-1} \cdot cm^{-1}$ for GrxS12 and Srx, respectively. GrxC5 (At4g28730) was purified following
113 established procedures [17,18].

2.4. Xylenol orange assay

115 The ferrous-dependent xylenol orange assay (FOX) was used to analyze the activity of PRX-IIE
116 and its phosphomimic variants with DTT as electron donor. The reaction mixture contained 2 µM
117 PRX-IIE and 4 mM dithiothreitol (DTT) in 40 mM K-Pi pH 7.2. The measurement was started by
118 addition of peroxides (400 µM H_2O_2, 200 µM t-BOOH or 200 µM CuOOH) in a time course of 90 sec
119 at 15 s intervals. The remaining peroxides were detected by ferrous-dependent oxidation of xylenol
120 orange as reported previously [19].

2.5. NADPH-dependent peroxidase activity measurement

122 Reduction of peroxides by PRX-IIE was monitored with the GRX system as reductant. The
123 activity was measured using a Cary 300 Bio UV/VIS spectrometer (Varian, Middelburg, Netherlands)
124 following NADPH oxidation at 340 nm. The assay was performed at 25 °C in quartz cuvettes with
125 2 µM PRX-IIE, 0.5 units glutathione reductase (GR), 200 µM NADPH, 1 mM EDTA, 1 mM GSH,
126 varying amounts of GrxS12 and of peroxides (H_2O_2, t-BOOH, CuOOH) in 40 mM K-Pi, pH 7.2.

2.6. Hyperoxidation of PRX-IIE

128 Hyperoxidation of PRX-IIE was assayed as described above using the FOX assay with 400 µM
129 H_2O_2 as substrate and increasing CuOOH concentrations. Furthermore, the oxidation state was
130 investigated by electrospray ionization coupled with mass spectrometry (ESI-MS; Esquire 3000,
131 Bruker Daltonics, Bremen, Germany). 10-20 µM of prereduced protein in 100 mM Tris-HCl, pH 8.0,
132 was incubated with 5 mM DTT and different CuOOH and 0.5 mM DTT and increasing H_2O_2
133 concentrations for 1 h at room temperature (RT). Excess low molecular weight reagents were
134 removed by acetone precipitation and proteins were resuspended in H_2O. Dilutions were prepared
135 in 30 % EtOH, 0.1 % formaldehyde (FA) and the mixture was introduced into the ESI-MS.
136 Instrumental settings: Capillary voltage = 4.000 V. Nebulizer gas pressure = 15 psi. Drying gas flow =
137 4.0 L/min. Drying gas temperature = 300 °C. Mass-to-charge (m/z) values: 650-1200. Mass spectra
138 were deconvoluted using the software provided by the manufacturer (DataAnalysis, Bruker
139 Daltonics, Bremen, Germany).

2.7. S-glutathionylation

141 10 – 30 µM PRX-IIE in 100 mM Tris-HCl, pH 8, was reduced for 30 min at room temperature
142 (RT) with 4 mM DTT. Desalting was achieved by passing the solution through PD10 columns. S-
143 glutathionylation was carried out by disulfide exchange with oxidized glutathione (GSSG) for 1 h at

144 RT. Excess GSSG was removed via acetone precipitation. Afterwards, S-glutathionylation was
145 detected by Western blot using monoclonal anti-GSH antibody (Thermo Scientific, Schwerte,
146 Germany). In addition, molecular masses of modified and unmodified proteins were assessed by ESI-
147 MS as mentioned before. For deglutathionylation, 10 µM glutathionylated PRX-IIE was incubated
148 with 10 µM of GrxS12, GrxC5 or SRX and 0.5 mM GSH at 25 °C. The decrease of glutathionylated
149 PRX-IIE was determined using Western Blot with anti-GSH antibodies. The spot intensities were
150 analysed using ImageJ.

151 *2.8. 2-Dimensional SDS-PAGE*

152 6-week-old *A. thaliana* Col_0 plants were sprayed with 300 µM methylviologen (MV) and 0.1%
153 (v/v) Tween-20 as control, respectively. After 3 h the plants were harvested and immediately frozen
154 in liquid nitrogen and grinded. Proteins were isolated and used for the separation in the first
155 dimension with Immobiline Dry Stripes (pH range 3-10 NL, 18 cm, GE Healthcare, Uppsala, Sweden)
156 [20]. To this end 250 µg protein were dissolved in 340 µL rehydration buffer (0.01% ampholyte;
157 0002 % (w/v) bromophenolblue) and applied to the Immobiline Dry Stripe. The rehydration and
158 focusing consisted of the following steps: 1 h 0 V, 12 h 30 V, 2 h 60 V, 1 h 500 V, 1 h 1000 V and 8000 V
159 until 42000 Vh were reached. Separation in the second dimension was done with 12 % non-reductive
160 SDS-PAGE. Afterwards, the gel was blotted to nitrocellulose membrane and subjected to Western
161 blotting with PRX-IIE antibody. and peroxidase-labeled secondary antibodies. Detection was done
162 with ECL Substrate (GE Healthcare, Chicago, IL, USA) and X-ray films.

163 *2.9. Subcellular localisation of PRX-IIE*

164 The open reading frame of PRX-IIE from *A. thaliana* was cloned into the 35S-EYFP-NosT vector
165 using specific primers (Table S1) for *in vivo* subcellular localization of PRX-IIE [21]. The resulting
166 construct consists of the PRX-IIE preprotein fused to EYFP as reporter under control of the CaMV35S-
167 promotor. Transient expression in mesophyll protoplasts and confocal laser scanning microscopy
168 were performed as described by Seidel et al. [22]. Chloroplast isolation and fractionation for
169 subplastidial Western blot analysis with antibodies raised against PRX-IIE were carried out according
170 to Muthuramalingam et al. [23].

171 *2.10. Affinitiy chromatographie and mass spectrometry*

172 Reduced His-tagged PRX-IIE (3 mg) or PRX-IIE C146S (3 mg) were bound to 1 mL Ni-NTA resin
173 (Qiagen, Hilden, Germany) and used as affinity matrix. Ni-NTA matrix without PRX-IIE served as
174 control. Leaves of about 5-week-old plants were homogenized in 50 mM Tris-HCl, pH 8.0, 1 mM
175 PMSF, filtrated through Miracloth. Clear protein extract was obtained via centrifugation (30 min at
176 20.000 rpm and 4°C). The supernatant (about 40 mg protein) was applied to the matrix and incubated
177 at RT with gentle agitation for 1.5 h. Non-bound material was removed by washing the column with
178 20 mL of 50 mM Tris-HCl, pH 8.0, and 20 mL of 50 mM Tris-HCl, pH 8.0, 200 mM NaCl. The first
179 elution step was achieved with 1 ml of 50 mM Tris-HCl, pH 8.0, 200 mM NaCl, 50 mM DTT and
180 incubation for 15 min at RT. The eluted fraction was collected and stored. Afterwards the columns
181 were washed with 10 mL 50 mM Tris-HCl, pH 8.0, 200 mM NaCl. During the second elution step the
182 material was incubated for 15 min at RT in 1 mL 50 mM Tris-HCl, pH 8.0, 200 mM NaCl, 50 mM DTT
183 and 500 mM imidazole. The samples of the first and second elution were trypsinated after
184 chloroform/methanol precipitation [24] and dissolved in 0.1 % TCA, 1 % acetonitrile. Peptides were
185 separated by reverse-phase nano LC and analyzed by electrospray ionization-mass spectrometry
186 (ESI-QTOF-MS) as described elsewhere [25]. Data were searched against the entries of UP000006548
187 3702 ARATH *A. thaliana* of the UniProt database using ProteinLynx Global Server 3.0.2. Proteins,
188 which were found in two out of three biological experiments with at least two peptides were accepted
189 for further analysis. In addition, proteins, which were identified in control sample (nonspecific
190 binding), were removed from protein lists. The LC-MS data are deposited using the e!DAL system of
191 IPK Gatersleben [26] and available at: the submission is under progress and will be available soon.

192 *2.11. Far Western blot*

193   Dilution series of recombinant 14-3-3 υ protein were spotted on nitrocellulose membrane,
194 together with a dilution series of PRX-IIE as calibration curve. The membrane was blocked with Tris-
195 buffered saline (TBS), pH 7.5, containing 1 % (w/v) milk powder. The membrane was incubated with
196 PRX-IIE or its phospho-mimicry variants in TBS with either 1 mM DTT or 100 μM H_2O_2 over night at
197 4°C. After three times washing with TBS for 5 min, proteins were detected using specific anti-PRX-
198 IIE antibody, peroxidase-labeled secondary antibody against rabbit, ECL® substrate (GE Healthcare,
199 Chicago, IL, USA) and X-ray films. Intensity quantification of the spots after documentation was done
200 using ImageJ. The relative amounts of bound PRX-IIE were determined in the linear range of the
201 blots.

202 *2.12. Structural modeling*

203   PRX-IIE structure was obtained from SWISS-MODEL [27] based on the structure of *Populus*
204 *tremula* PRX D type II (pdb: 1tp9A). Further analysis was done with PyMOL version 2.4.0 [28].

205 **3. Results**

206 *3.1. PRX-IIE is localized to the chloroplast stroma*

207   The PRX family in *A. thaliana* consists of 10 ORFs, of which 9 members are described to be
208 expressed [29]. Besides the mitochondrial PRX-IIF, RRX-IIE is the only type II PRX in Arabidopsis
209 which displays a putative transit peptide. Bioinformatic analysis of the preprotein sequence predicted
210 an N-terminal chloroplastic transit peptide for the first 70 amino acids (Figure 1A). The remaining
211 amino acids form the stable TRX-like structure with seven β-sheets and five α-helices (Figure 1B). To
212 study the subcellular localization of PRX-IIE, a plasmid encoding the PRX-IIE-EYFP fusion protein
213 was transfected into mesophyll protoplasts. Confocal laser scanning microscopy of the transfected
214 protoplasts revealed the plastidial localization, as indicated in the overlay of the EYFP signal with
215 the chlorophyll autofluorescence (Figure 1C). Western blot analysis of fractionated chloroplasts with
216 anti-PRX-IIE antibody revealed a signal exclusively in the stromal fraction, whereas the
217 thylakoid/membrane fraction lacked any PRX-IIE signal (Figure 1D).

218

219
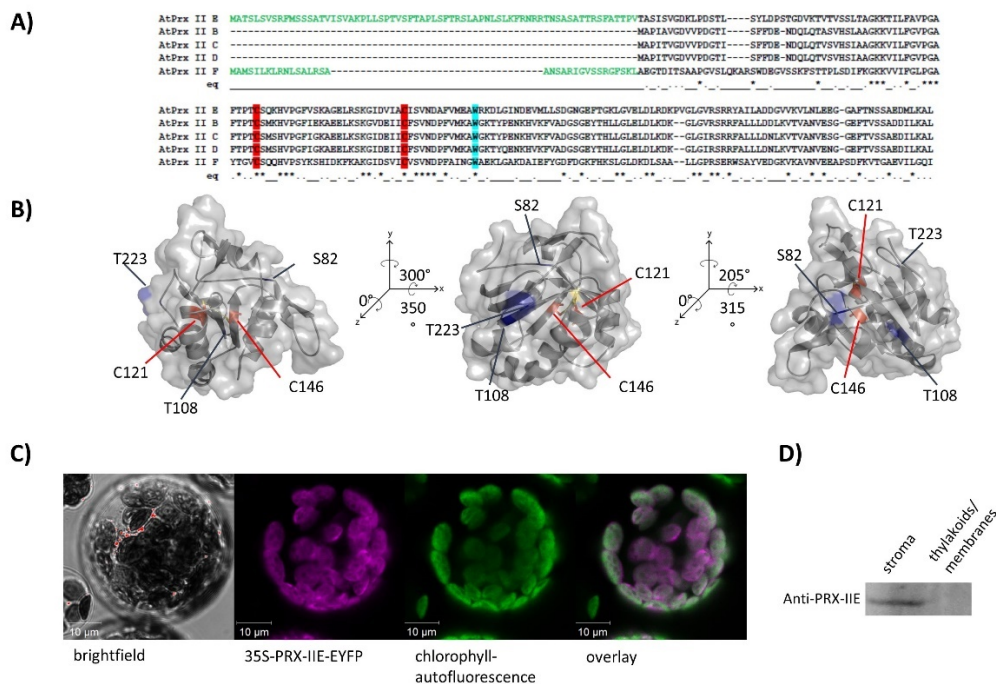
220 **Figure 1 Subcellular localization of PRX-IIE.** A) Amino acid sequence alignment of *A. thaliana* type
221 II PRXs. The signal peptides of PRX-IIE and PRX-IIF are highlighted in green as well as the highly

222 conserved cysteines (C: red) and tryptophan (W: blue). B) Predicted 3D structure of mature PRX-IIE
223 from three different points of view. The model is based on the PRX D type II from *P. tremula*
224 (pdb:1tp9A) and further analysis was done using PyMOL 2.4. Both cysteines, C121 and C146 are
225 marked in red, whereas the possible phosphorylation sites S82, T108 and T223 are marked in blue.
226 The distance between the cysteines are 7.83 Å. The accessible surface area of the peroxidatic cysteine
227 at position 121 is 0.795 Å^2. C) The coding sequence of PRX-IIE was fused in frame to EYFP as reporter
228 and used for transient expression in *A. thaliana* mesophyll protoplasts. Confocal laser scanning images
229 reveal chlorophyll autofluorescence (green) and fluorescence of the PRX-IIE-EYFP construct (purple).
230 White areas in the overlay indicate chloroplastic localization of PRX-IIE. D) Subplastidal localization
231 of PRX-IIE was analyzed in isolated intact chloroplasts fractionated into stroma and membrane
232 fraction by ultracentrifugation. Equal amounts of both fractions (50 µg protein) were loaded per lane
233 and PRX-IIE was identified in chloroplast stroma using specific anti PRX-IIE antibody.

234 *3.2. PRXIIE detoxifies H_2O_2 using the GRX system for regeneration*

235 Peroxiredoxins reduce a broad range of peroxides and their activities rely on the conserved
236 cysteine residues. Reduction of H_2O_2 by PRX-IIE and its cysteine variants was determined using the
237 FOX assay. The removal of either the Cys_P as well as the Cys_R residue has a negative impact on
238 peroxidase activity, constraining that both thiol groups are necessary for reactive oxygen species
239 (ROS) scavenging (Figure 2A). Substrate specificity with H_2O_2, t-BOOH and CuOOH of wild-type
240 (WT) protein is depicted in Figure 2B. PRX-IIE showed the highest rate of activity with H_2O_2 as
241 substrate and DTT as reductant. Reduction rates of t-BOOH and CuOOH relative to H_2O_2 were about
242 20 % and 0.5 %, respectively. This indicates that H_2O_2 is the preferred substrate for PRX-IIE.
243 Furthermore, peroxide reduction by PRX-IIE in the presence of chloroplastic glutaredoxin-S12 (GRX-
244 S12) as reductant was determined (Figure 2C) and confirmed H_2O_2 as preferred substrate, but unlike
245 with DTT, lower activities were recorded.
246
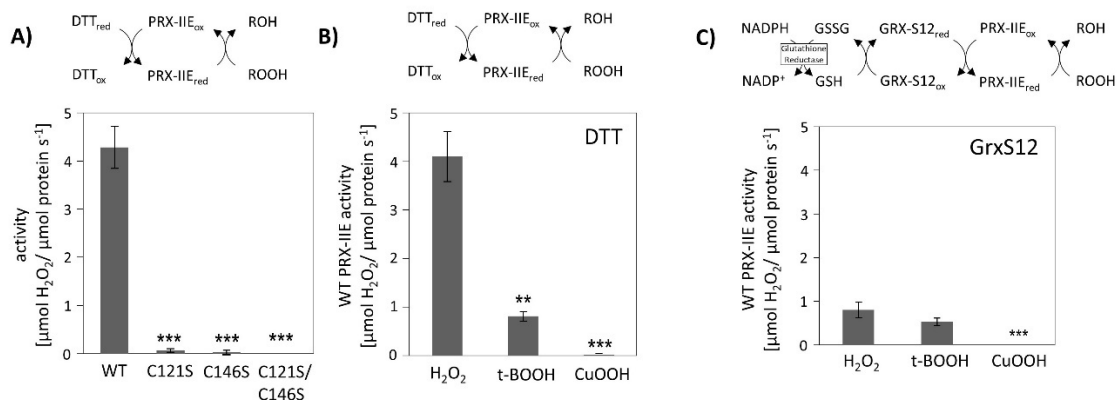
248 **Figure 2 Peroxidase activity.** A) Peroxide reduction by wild-type PRX-IIE and its cysteine variants
249 was measured with 400 µM H_2O_2, 4 mM DTT and 2 µM protein. The decrease in H_2O_2 was quantified
250 with the FOX assay. Data are means ± SD, n = 30 with protein of three independent protein
251 purifications. ***: p < 0.001. B) Substrate specificity was tested with the FOX assay with 4 mM DTT as
252 reductant and different peroxides (400 µM H_2O_2, 200 µM t-BOOH or 200 µM CuOOH). Data are
253 means ± SD, n = 18-28 with protein from three independent protein purifications. **: p < 0.01; ***: p <
254 0.001. C) PRX-IIE activity in the presence of GRX-S12 as monitored as NADPH oxidation at 340 nm
255 in an enzyme-coupled reduction. Data are means ± SD, n = 9 with protein from three independent
256 protein purifications. **: p < 0.01; ***: p < 0.001.

257 *3.3. CuOOH- and H_2O_2-dependet hyperoxidation*

258 CuOOH is a strong oxidizing agent and based on activity measurements (Figure 2B) it was
259 assumed that PRX-IIE is hyperoxidized by CuOOH. This hypothesis was tested *in vitro* using the FOX
260 assay at increasing CuOOH concentrations (Figure 3A). A significant inhibition of H_2O_2 detoxification

261 could be detected in the presence of 12.5 µM CuOOH and the peroxidase activity was undetectable
262 at high CuOOH concentration. To further address the possibility for overoxidation of PRX-IIE by
263 CuOOH, ESI-MS analysis was carried out (Figure 2 B). In contrast to reduced PRX-IIE with a
264 molecular mass of 19438.0 Da, the sample treated with 0.5 mM CuOOH showed a mass increase of
265 ~32 Da which corresponds to the formation of the sulfinic acid derivative ($-SO_2H$). Higher CuOOH
266 concentrations lead to further oxidation to the sulfonic acid ($-SO_3H$).
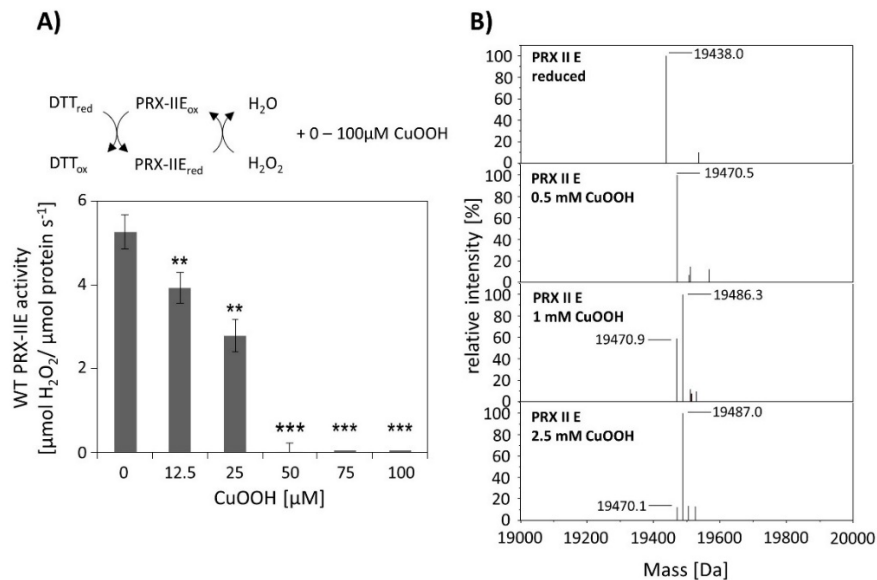
268 **Figure 3 Hyperoxidation of PRX-IIE.** A) Activity of 2 µM PRX-IIE was determined with 400 µM H_2O_2
269 as substrate and 4 mM DTT using the FOX assay. CuOOH concentrations >50 µM completely
270 inhibited the peroxidase activity. Data are means ± SD, n = 9 with protein of three independent protein
271 purifications. **: p < 0.01; ***: p < 0.001. B) Deconvoluted ESI-MS spectra of wild-type PRX-IIE after
272 treatment with CuOOH as described in Materials and Methods. 19438.0 is the expected mass of the
273 reduced (-SH), His-tagged PRX-IIE protein. The peak at 19470.5 Da after incubation with 0.5 mM
274 CuOOH shows a mass increase by 32 Da, which corresponds to the formation of the sulfinic acid
275 derivative ($-SO_2H$). Higher CuOOH concentrations lead to further oxidation to the sulfonic acid
276 ($-SO_3H$). Data are representative spectra of n = 15 measurements with protein of three independent
277 protein purifications.

278 ESI-MS analysis of cysteine variants of PRX-IIE was performed to elucidate which of the two
279 cysteines was modified (Table 1). Deconvoluted data revealed that hyperoxidation occurs in the
280 C146S variant, lacking the Cys_R, while the PRX-IIE protein variant lacking Cys_P (C121S) showed only
281 a slight oxidation at high CuOOH concentrations.

282 **Table 1 CuOOH-dependent thiol modifications of PRX-IIE variants.** Proteins were treated with
283 DTT and CuOOH for 1 h at RT and then analyzed by ESI-MS. Generation of the oxidized (-SOH) and
284 hyperoxidized ($-SO_2H$, $-SO_3H$) forms increased the mass of the protein by 16, 32 or 48 Da. Data are
285 means ± SD, n = 10 with protein from two independent purifications.

Treatment	PRX-IIE C121S		PRX-IIE C146S	
	Mass [Da]	Cys modification	Mass [Da]	Cys modification
5 mM DTT (control)	19,422.93 ± 0.61	None (SH)	19,422.22 ± 0.52	None (SH)
0.5 mM CuOOH	19,422.75 ± 0.57	None (SH)	19,422.57 ± 0.55	None (SH)
			19,454.61 ± 0.44	Hyperoxidation (SO_2H)
1 mM CuOOH	19,423.13 ± 0.22	None (SH)	19,422.86 ± 0.87	None (SH)
			19,454.93 ± 0.62	Hyperoxidation (SO_2H)
2.5 mM CuOOH	19,423.31 ± 0.17	None (SH)	19,422.46 ± 0.86	None (SH)
			19,454.51 ± 0.92	Hyperoxidation (SO_2H)
			19,471.37 ± 0.81	Hyperoxidation (SO_3H)
5 mM CuOOH	19,422.95 ± 0.54	None (SH)	19,422.52 ± 0.41	None (SH)
			19,453.86 ± 0.53	Hyperoxidation (SO_2H)
			19,470.75 ± 0.96	Hyperoxidation (SO_3H)
10 mM CuOOH	19,422.97 ± 0.57	None (SH)	19,423.25 ± 0.69	None (SH)
	19,438.11 ± 0.92	Oxidation (SOH)	19,454.14 ± 0.98	Hyperoxidation (SO_2H)
			19,470.73 ± 0.81	Hyperoxidation (SO_3H)

Activity measurements for PRX-IIE revealed that H_2O_2 is the preferred substrate (Figure 2B), but H_2O_2 is also known to catalyze hyperoxidation of proteins [18]. To test this for PRX-IIE, peroxide-mediated hyperoxidation was analyzed by ESI-MS (Figure 4). The extent of sulfinic acid formation was tentatively estimated from the ratio of the peak intensities for the reduced (-SH, 19438.0 Da) and hyperoxidized (-SO_2H, 19470.0 Da) protein in the deconvoluted ESI-MS spectra. Incubation of PRX-IIE with 25 µM H_2O_2 resulted in an hyperoxidation rate of 46 %, and higher peroxide concentrations lead to further hyperoxidation of the protein. Masses that correspond to the sulfonic acid (-SO_3H) could not be detected, suggesting that H_2O_2-mediated hyperoxidation is limited to the formation of the sulfinic acid derivative at Cys_P.
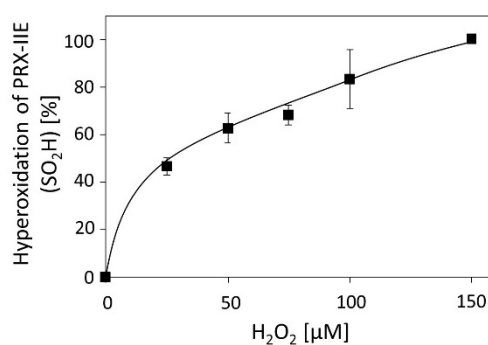

Figure 4 H_2O_2-dependent hyperoxidation of PRX-IIE. The extent of sulfinic acid formation in percent of total was estimated from the ratio of the peak intensities for the reduced (SH; 19.438 Da) and hyperoxidized (SO_2H; 19.470 Da) protein in the deconvoluted ESI-MS spectra. Data are means of n = 10 ± SD with recombinant protein from two independent purifications.

3.4. S-Glutathionylation of PRX-IIE occurs at Cys_p

The results shown above revealed a lower peroxidase activity for PRX-IIE with GRXs as electron donor in comparison to DTT as reductant (Figure 2C). The antioxidant glutathione is one component

305   of the assay. In addition, H_2O_2-dependent hyperoxidation of PRX-IIE could be observed (Figure 4).
306   For *A. thaliana* and *T. brucei* reversible S-glutathionylation, the addition of one glutathione molecule
307   to specific cysteine residues, has been shown to prevent 2-Cys PRX to hyperoxidize and thereby
308   regulates its function [30,31]. In order to analyze the possibility for this redox-related
309   posttranslational modification, reduced PRX-IIE was incubated with either 0.5 mM DTT or 10 mM
310   oxidized glutathione (GSSG) overnight at 4°C. Following acetone precipitation samples were
311   subjected to ESI-MS and intact masses of the protein were obtained (Figure 5)
312
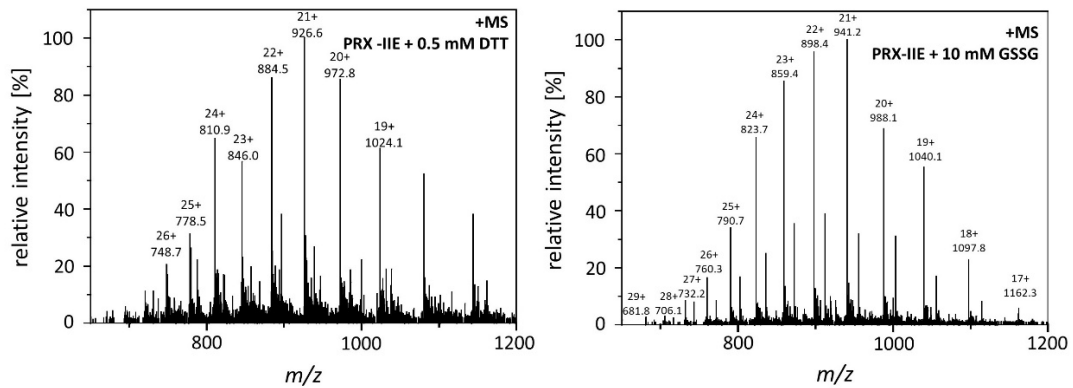
313

314   **Figure 5 Mass spectra of reduced and S-glutathionylated PRX-IIE.** S-glutathionylation was carried
315   out by disulfide exchange with GSSG. The reaction mixtures containing 30 μM reduced PRX-IIE
316   without (left diagram) or with 10 mM GSSG (right diagram) in Tris buffer, pH 8.0, were incubated at
317   4°C for 18 h. The protein products were precipitated and subsequently subjected to ESI-MS analysis.

318   Deconvoluted data revealed the addition of one glutathione residue that increased the mass of
319   the protein by 306 Da (Figure 6A). The PTM of PRX-IIE was further proven with specific anti-GSH
320   antibody (Figure 6B). In addition, S-glutathionylation of PRX-IIE at low physiological GSSG
321   concentrations could be observed (Figure 6A). The time-dependent S-glutathionylation *in vitro* was
322   detected after incubation with GSSG for different time periods (Figure 6C). Thiol modification was
323   observed already after 10 min and reached a maximum at 60 min. The results demonstrate the fast S-
324   glutathionylation of PRX-IIE at physiological relevant concentrations *in vitro*. Not only incubation of
325   PRX-IIE with GSSG results in S-glutathionylation, but also incubation of pre-reduced PRX-IIE with
326   1 or 5 mM S-nitrosoglutathione. Besides this, formation of N-nitrosation (19.469 kDA, -SNO) and S-
327   nitrosoglutathionylation (19.772 kDa, -SSGNO) was observed, using ESI-MS.
328
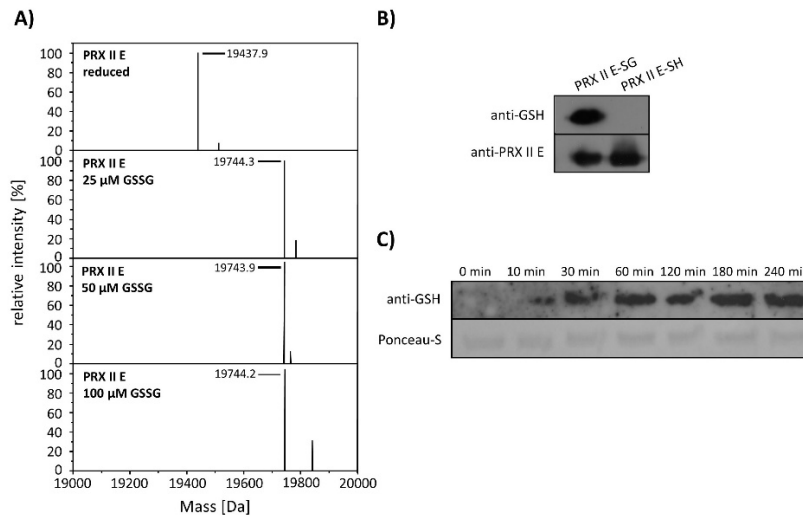
Figure 6 S-glutathionylation of PRX-IIE. A) Deconvoluted mass spectra of reduced and S-glutathionylated PRX-IIE after treatment with oxidized glutathione (GSSG). Reduced PRX-IIE (19,438 Da) was treated with indicated GSSG concentrations and the degree of modification was estimated from the mass shift of 306 Da to 19744 Da, which could be assigned to monoglutathionylated protein. Data are representative spectra of n = 12, with protein from three independent protein purifications. B) Western blot analyses of reduced and S-glutathionylated PRX-IIE (treatment with 10 mM GSSG) using specific anti-GSH and anti-PRX-IIE antibody. C) Time dependence of S-glutathionylation with recombinant PRX-IIE *in vitro*.

To test for the particular residue that is prone to S-glutathionylation, Cys to Ser variants were analyzed using Western Blot with specific anti-GSH antibody. Results showed S-glutathionylation of WT PRX-IIE and the C146S variant, but not on the C121S variant (Figure 7). Furthermore, mass spectrometry was done with the WT and the Cys→Ser variants. 19422 Da correspond to the reduced variants with single mutated cysteine residues (C121S or C146S) and 19406 Da to the double mutant. Only the C146S protein, lacking the Cys_R at position 146, was S-glutathionylated in a concentration-dependent manner of GSSG (Figure 7B).
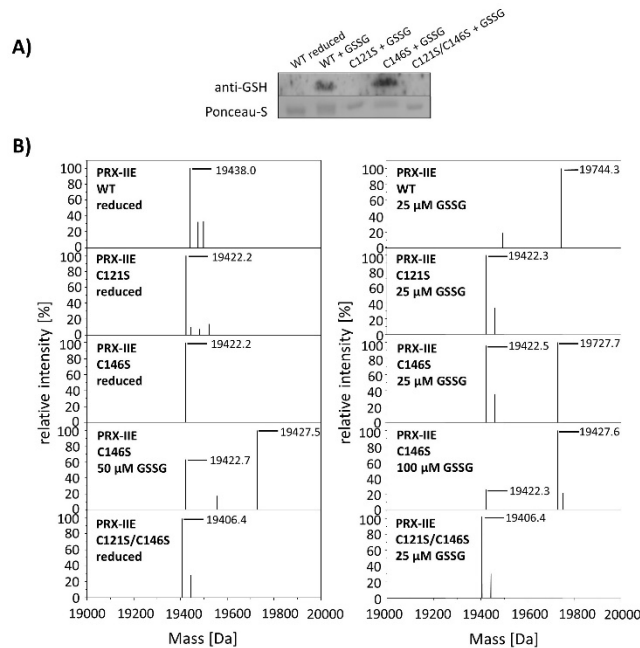

Figure 7 Identification of S-glutathionylated Cys residue in PRX-IIE using Cys→Ser variants. To test for the site of glutathionylation, Cys→Ser mutated PRX-IIE variants were analyzed by Western

349   blot with specific anti-GSH antibody and by mass spectroscopy. A) 10 µM reduced WT PRX-IIE and
350   variants (C121S; C146S; C121S/C146S) were incubated with 10 mM GSSG for 1 h at RT and subjected
351   for Western blot analysis. B) Representative deconvoluted ESI-MS spectra of PRX-IIE and variants
352   treated with GSSG. 19438 Da corresponds to the theoretical mass of the reduced and His-tagged
353   protein, whereas a shift of 306 Da to 19744 was observed for the glutathionylated version of PRX-IIE
354   with a single bound glutathione molecule. 19422 Da correspond to the reduced variants with single
355   mutated cysteinyl residues (C121S; C146S) and 19406 Da to the double mutant. Only the C146S
356   protein, lacking the Cys_R, was glutathionylated in a concentration-dependent manner. The figure
357   shows representative spectra of n = 6 determinations, using two independent protein purifications.

358   Next, the effect of S-glutathionylation on peroxidase activity was investigated using a modified
359 FOX assay (Figure 8A). Peroxidase activity in the presence of GRX-S12, GSH and H_2O_2 as substrate
360 decreased in the presence of GSSG amounts as low as < 2.5 % GSSG of total glutathione. The extent
361 of glutathionylation was tested by ESI-MS at different GSH/GSSG ratios (Figure 8B). Deconvoluted
362 spectra showed the presence of PRX-IIE-SG already at 1.25 % GSSG, which is in line with the
363 decreased peroxidase activity. Protein-SG forms through several mechanisms *in vitro*, however the
364 precise reaction mechanism *in vivo* remains unclear [32]. In contrast, deglutathionylation reaction is
365 reported to be catalyzed by GRXs and SRXs [33,34]. To monitor the deglutathionylation of PRX-IIE,
366 PRX-IIE-SG was incubated with GSH in the presence or absence of GRX-S12, GRX-C5 and SRX
367 (Figure 8C). Western blot analysis with specific GSH antibody revealed a decrease in signal intensity
368 for PRX-IIE-SG after 20 min of reaction time with GSH alone. The addition of SRX or GRX did not
369 increase the deglutathionylation reaction, leading to the conclusion that the glutathione pool itself is
370 capable of modulating the redox state of PRX-IIE.
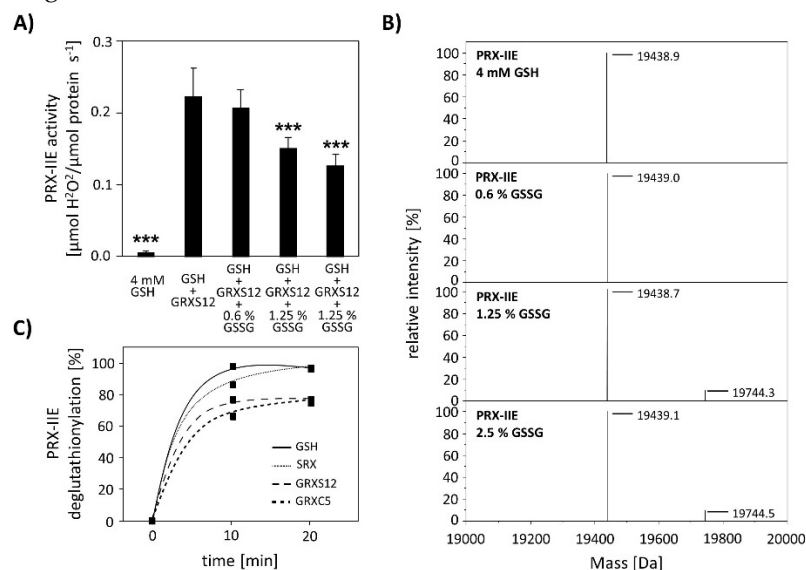
372 **Figure 8 Effect of glutathionylation on peroxidase activity and deglutathionylation reaction.** A)
373   Titration of peroxidase activity of PRX-IIE in the presence of GRX-S12, GSH and H_2O_2 and increasing
374   amounts of GSSG using the FOX assay. Glutathionylation and inhibition of activity occured at <2.5 %
375   GSSG of total glutathione. Data are means of n=10 ± SD with protein of two independent protein
376   purifications; *** $p \leq 0.001$. B) PRX-IIE was treated with different GSH/GSSG ratios and
377   glutathionylation was determined via ESI-MS. Deconvoluted spectra reveal the presence of
378   glutathionylated PRX-IIE already at 1.25 % GSSG. (C) Time course of the deglutathionylation reaction.
379   10 µM PRX-IIE-SG were incubated together with 0.5 mM GSH and equal amounts of sulfiredoxin
380   (SRX), GRX-S12 or GRX-C5 in 100 mM Tris-HCl, pH 8.0, at 37 °C for indicated time and the decrease
381   in signal intensity was monitored over time using anti-glutathione antibody.

382   Protein S-glutathionylation ensures protection of critical protein thiols against irreversible
383 overoxidation *in vivo* and is therefore considered as biomarker for oxidative stress [35,36]. To test
384 redox-dependent posttranslational modifications of PRX-IIE *in vivo*, *A. thaliana* plants were sprayed

385 with a single dose of 300 μM methylviologen, harvested after 3 h and analyzed using non-reducing
386 two-dimensional gel electrophoresis following Western blot with specific anti-PRX-IIE antibody. In
387 contrast to the mock treated samples, which showed two protein spots representing reduced (-SH)
388 and presumably oxidized protein species, plants stressed with MV exhibited three distinct protein
389 spots, two of them differed in acidity and molecular mass (Figure 9). Mature PRX-IIE-SH displays a
390 molecular mass of 17260 Da with a theoretical pI value of 5.02, whereas for PRX-IIE-SG a mass shift
391 to 17566 Da and a more acidic pI value of 4.91 are predicted. Molecular mass and pI values were
392 obtained using the Expasy ProtParam tool [37]. Theoretical pI calculations and correlation with the
393 pI values observed on the 2D gels together with the mass change, suggest that the acidic spots of the
394 triplet correspond to the glutathionylated protein.

395
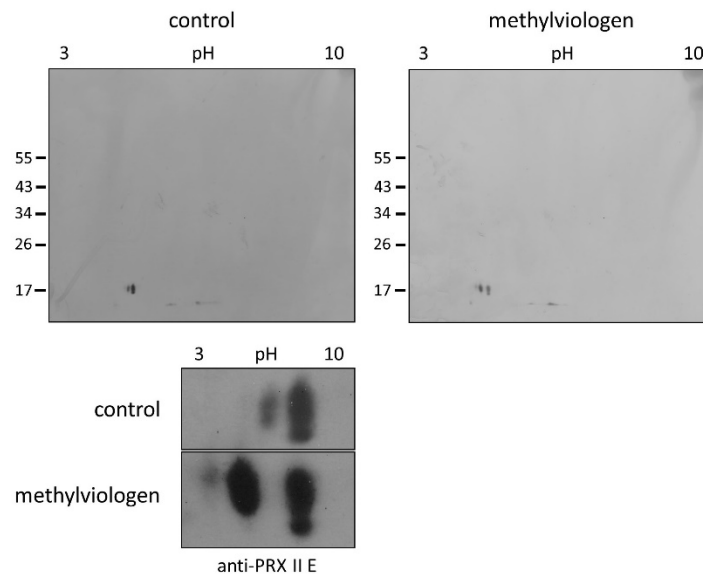
Figure 9 Detection of glutathionylated PRX-IIE species *in vivo*. *A. thaliana* plants were stressed for
3 h with 300 μM MV or 0.1 % (v/v) Tween-20 as control. S-glutathionylation was detected with specific
anti-PRX-IIE antibody following separation by non-reducing 2D-SDS-PAGE and blotting. The figure
shows representative Western blots from two independent experiments.

3.5. Identification of PRX-IIE interaction partners

401 The next experiments aimed to elucidate, whether PRX-IIE exclusively functions as a peroxidase
402 or if it might be involved in cell signaling by direct protein-protein interactions. For that, an affinity
403 chromatography approach with immobilized His$_6$-tagged PRX-IIE and total *A. thaliana* leaf protein
404 was used to identify interacting proteins. After washing, bound proteins were eluted with buffer
405 containing DTT or imidazole. They were subsequently identified by mass spectrometry. In addition,
406 a thiol-trapping experiment with the C146S variant was used in order to identify redox-regulated
407 proteins that preferentially interact through the Cys$_P$. The reductive elution with DTT resulted in the
408 identification of 47 proteins, 14 of which were also identified to interact with the C146S variant
409 (Figure 10A). To address proteins that interact with PRX-IIE electrostatically, a second elution was
410 done with imidazole. Seven proteins co-eluted with PRX-IIE, and 9 with the PRX-IIE C146S variant
411 (Figure 10B). Out of the 54 proteins that interacted with PRX-IIE, 24 are localized within the
412 chloroplast and half of them are involved in metabolic pathways (Figure 10C). However, in
413 comparison to the WT protein, almost the same number of proteins were trapped by the C146S
414 variant, but only 14 of them reside in the chloroplast (Figure 10D).
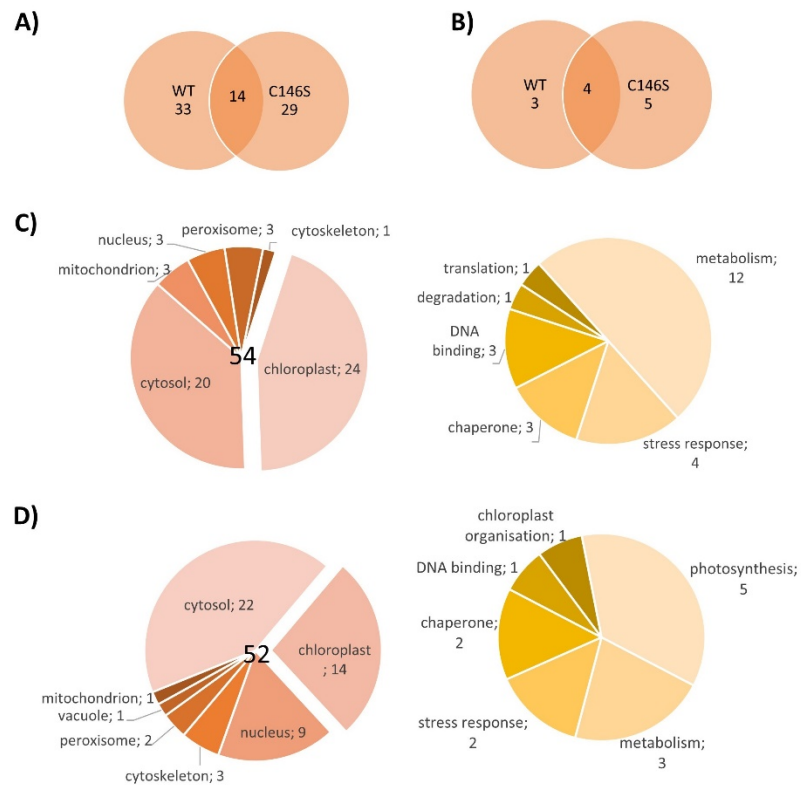
Figure 10 Localization and function of PRX-IIE interaction partners. Venn diagrams depicting unique and overlapping interactors of PRX-IIE WT and C146S variant after A) elution with DTT and B) second elution with imidazole. Identified interacting proteins with C) PRX-IIE WT or D) PRX-IIE C146S during first and second elution, were grouped according to their localization and function. See also supplementary file.

Interestingly, 4 out of the 24 identified chloroplast proteins trapped by the WT PRX-IIE protein belong to the 14-3-3 family (Table 2). In total 6 different 14-3-3 proteins were identified regardless of the bait protein (Table S 2). Plant 14-3-3 proteins are reported to be involved in multiple developmental and stress related processes, such as apoptosis, leaf shape and salt stress tolerance [38–40]. They normally occur as homodimers or heterodimers and are able to bind two different targets at the same time and, therefore, act as scaffold proteins [41]. Furthermore, they are involved in signaling processes regulated by phosphorylation [42–44]. Since PRX-IIE has three experimentally reported phosphorylation sites [45], an interaction between PRX-IIE and a 14-3-3 protein could be part of a signaling process. To study the interaction between PRX-IIE and 14-3-3 proteins in more detail, 14-3-3 υ was chosen as a representative for the 14-3-3 protein family and used in further experiments.

Table 2 Chloroplast localized interaction partners of PRX-IIE WT. Listed are the proteins identified from elution with DTT (above the line) and imidazole (below the line), with AGI code and uniport accession number

AGI code	Protein accession	Protein name
AT4G09000	P42643	14-3-3 χ
AT5G10450	P48349	14-3-3 λ
AT3G02520	Q96300	14-3-3 ν
AT5G16050	P42645	14-3-3 υ
AT3G60880	Q9LZX6	4-Hydroxy-tetrahydrodipicolinate synthase 1
AT1G02560	Q9S834	ATP-dependent Clp protease proteolytic subunit 5
AT5G03690	F4KGQ0	Fructose-bisphosphate aldolase 4
AT4G26530	O65581	Fructose-bisphosphate aldolase 5

|		
AT5G49910	Q9LTX9	Heat shock 70 kDa protein 7
AT2G24200	P30184	Leucine aminopeptidase 1
AT5G45930	Q5XF33	Magnesium-chelatase subunit ChII-2
AT1G70890	Q9SSK5	MLP-like protein 43
AT5G26000	P37702	Myrosinase 1
AT3G62030	P34791	Peptidyl-prolyl cis-trans isomerase CYP20-3
AT2G29630	O82392	Phosphomethylpyrimidine synthase
AT5G52920	Q9FLW9	Plastidial pyruvate kinase 2
AT1G32440	Q93Z53	Plastidial pyruvate kinase 3
AT5G52520	Q9FYR6	Proline tRNA ligase
AT2G21170	Q9SKP6	Triosephosphate isomerase
AT4G17090	O23553	β-amylase 3
AT3G01500	P27140	β-carbonic anhydrase 1
AT5G14740	P42737	β-carbonic anhydrase 2
AT5G64460	Q9FGF0	Phosphoglycerate mutase-like protein 1

435

436   To characterize the interaction between 14-3-3 υ and PRX-IIE, phospho-mimicry variants of PRX-
437 IIE were generated and their peroxidase activity was analyzed using the FOX-Assay. Interestingly,
438 all variants revealed lower peroxidase activity in comparison to WT PRX-IIE, whereas S82D and
439 T108E showed a significant lower activity (Figure 11A). Binding between PRX-IIE or its
440 phosphomimic variants and 14-3-3 υ under defined redox-conditions conditions was assessed in an
441 overlay approach (Figure 11B). Binding was similar under all conditions apart from the 2.5-fold
442 improved binding of WT PRX-IIE to 14-3-3 υ under oxidizing conditions (Figure 11B).
443 Supplementation with 14-3-3 υ had a beneficial effect on peroxidase activity albeit a five-fold excess
444 of 14-3-3 υ was necessary to observe a significant increase of PRX-IIE peroxidase activity (Figure 11C).

445
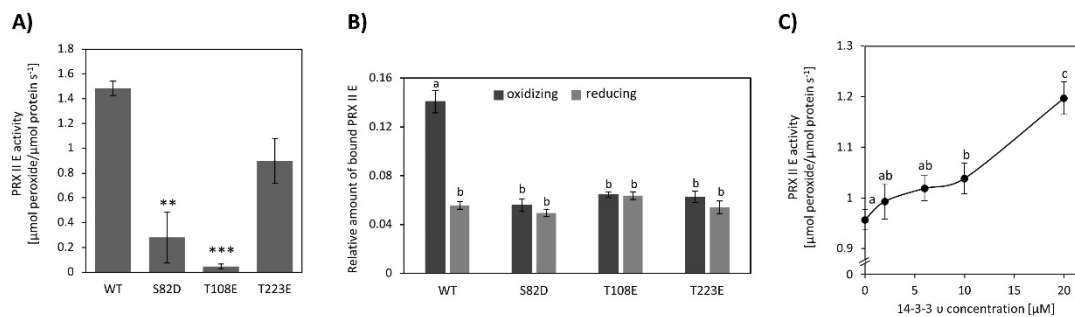
446 **Figure 11 Influence of phospho-mimicry point-mutations on the activity of PRX-IIE and the**
447 **interaction with 14-3-3 υ.** A) Peroxide reduction by wildtype PRX-IIE and its phospho-mimicry
448 variants were measured with 400 μM H_2O_2, 4 mM DTT and 2 μM protein. The decrease in H_2O_2 was
449 quantified with the FOX assay. Data are means of n = 10-16 ± SE with protein from three independent
450 protein purifications. Significant differences to the WT protein were calculated using Student T-Test
451 whereas **: $p < 0.01$; *** $p < 0.001$. B) Overlay assay of 14-3-3 υ with PRX-IIE. A higher affinity of PRX-
452 IIE to 14-3-3 υ was observed under oxidizing conditions. Data are means of n = 13-22 ± SD. Significant
453 differences were calculated using Student T- Test and are indicated by different letters $p \leq 0.05$. C)
454 Influence of 14-3-3 υ on the peroxidase activity of PRX-IIE. The activity of PRX-IIE was measured in
455 the presence of different concentrations of 14-3-3 υ with FOX Assay. Data are means of n= 12-18 ± SE.
456 Different letters indicate significant differences calculated with Student T-Test at $p \leq 0.05$.

457

4. Discussion

PRX-IIE is a thiol dependent peroxidase that is localized to the chloroplast stroma (Figure 1C, D). Two cysteinyl residues are highly conserved within the type II PRX (Figure 1A) and mutation of either one or both cysteines to serine results in a loss of peroxidase activity (Figure 2A). Therefore, both Cys, namely Cys_P121 and Cys_R146, are essential for the PRX-IIE peroxidase activity.

The human homologue peroxiredoxin 5 (PRDX5) more readily reduces t-BOOH [46], while PRX-IIE from *A. thaliana* showed the highest activity with H_2O_2 as substrate (Figure 2B, C). The differences in substrate specificity could be due to the different accessible surface areas of Cys_P of both enzymes. The accessible surface area of the Cys_P of PRDX5 is 1.305 $Å^2$, whereas the accessible surface area of the PRX-IIE Cys_P is just 0.795 $Å^2$ (Figure 1B). Therefore, PRX-IIE seems more likely to detoxify smaller peroxides in comparison to the human analogue PRDX5.

4.1. Regeneration of reduced PRX-IIE limits catalytic turnover

The GRX-S12-coupled assay revealed the same substrate preference as the FOX assay, however, the catalytic activities were lower in comparison to the DTT-driven activity, especially in case of H_2O_2 as substrate (Figure 2C). Since activity measurements with t-BOOH showed almost the same values, it seems that PRX-IIE regeneration by GRX-S12 is the rate-limiting step in the catalytic cycle of peroxide reduction, disulfide formation and regeneration.

4.2. Bulky substrates favour hyperoxidation and inhibition of PRX-IIE

Activity was undetectable in both assays using CuOOH as substrate, and rather bulky substrates like CuOOH inhibit peroxidase activity, which was already reported for *poplar* PRX-IIE [14]. The inhibitory effect of CuOOH on the peroxidase activity of PRX-IIE was revealed by the decreased H_2O_2-reduction activity in the presence of increasing CuOOH concentrations. Already the presence of 12.5 µM CuOOH resulted in a significant decrease in PRX-IIE peroxidase activity (Figure 3A) and the inhibition of activity correlated with hyperoxidation of PRX-IIE (Figure 3B).

ESI-MS measurements of CuOOH-treated PRX-IIE C121S and C146S variants proved hyperoxidation of the C121 to sulfinic ($-SO_2H$) and sulfonic acid (SO_3H) at low amounts of CuOOH (Table 1). Oxidation of C146 to sulfenic acid (-SOH) only occurred after treatment with relatively high CuOOH concentrations. H_2O_2 treatment only resulted in oxidation of PRX-IIE to the sulfenic acid derivative in contrast to 2-CysPRX, where hyperoxidation occurs after about 250 peroxidase cycles (Figure 4) [47]. Oxidized sulfenylated 2-CysPRX functions in proximity-based oxidation. Sobotta et al [48] reported this type of signaling cascade, where human PRDX2 gets oxidized by ROS and afterwards oxidizes STAT3. Disulfide-bonded 2-CysPRX from *A. thaliana* oxidizes chloroplast TRXs which in turn oxidize target proteins in the Calvin-Benson cycle or malate dehydrogenase [8]. This type of regulation was termed TRX oxidase function of 2-CysPRX and participates in adjustment of enzyme activity to decreased light intensity. PRX-IIE could also be part of a ROS-induced signaling cascade, whereas PRX-IIE oxidizes a nearby protein.

Hyperoxidized PRX may also function in cell signaling, e.g. if the change in redox-state affects its conformational state which in turn allows for binding to other proteins and alters their activity [49]. Pea mitochondrial PRX-IIF adopts a hexameric conformation in addition to its dimeric form and tightly binds thioredoxin-o [50].

4.3. Besides hyperoxidation, Cys121 of PRX-IIE is subject to multiple posttranslational modifications

Apart from oxidation and hyperoxidation, PRX-IIE is also S-glutathionylated (Figure **5** and Figure 6). Although glutathionylation of PRX-IIE inhibited its peroxidase activity (Figure 8A), S-glutathionylation of Cys_P (Figure 7) may prevent PRX-IIE from hyperoxidation, like it was already shown for glyceraldehyde-3-phosphate-dehydrogenase (GAPDH) from spinach and isocitrate lyase from *C. reinhardtii* [51,52]. Reversal of this type of regulation of PRX-IIE could be achieved by deglutathionylation via GRXs, TRXs and SRXs [53–55]. However, the presence of GRX-S12, SRX or

505 GRX-C5 failed to increase the deglutathionylation rate in comparison to GSH alone, indicating that
506 the GSH/GSSG ratio could be the main route for the regulation of this PTM *in vivo*.
507   Under normal physiological relevant concentrations of ~1 mM glutathione [56] and a ratio of
508 0.002 % oxidized glutathione [57], PRX-IIE should not be glutathionylated. Application of stresses to
509 the plant, like exposure to methylviologen or arsenic treatment can, however, alter the GSSG ratio
510 [58,59] and, therefore, may result in S-glutathionylation of PRX-IIE. This is consistent with the results
511 shown in Figure 9, where application of severe stress resulted in S-glutathionylation of PRX-IIE. This
512 post-translational modification could prevent PRX-IIE from hyperoxidation. In addition, reversible
513 S-glutathionylation of PRX-IIE could take part in PRX-dependent signal transduction and regulation
514 of the redox homeostasis [60].

515 *4.4. PRX-IIE binds to target proteins*

516   Besides post-translational control of activity, protein-protein interactions alter functions and
517 properties of binding partners. PRX-IIE protein interactions mostly seem to be redox-regulated, since
518 most of the trapped proteins were eluted with DTT (Figure 10A, B). In total 54 proteins were
519 identified to interact with PRX-IIE. Since PRX-IIE is located in plastids, we focused on the 24 proteins
520 with plastidial localization. However also the other proteins deserve attention since they might
521 interact with the cytosolic type II PRXs which display high similarity with PRX-IIE (Figure 1A). Most
522 of the identified proteins are known targets of redox regulation [61] like cyclophilin 20-3 [55] or β-
523 carbonic anhydrase [62].

524 *4.5. 14-3-3 proteins as binding partner of PRX-IIE open up new perspectives*

525   14-3-3 proteins function as molecular adapters and their identification as binding partners of
526 PRX-IIE appeared interesting and novel. They are present in various isoforms in plant genomes and
527 act as homo- and heterodimers [63]. 14-3-3 proteins are able to integrate and control multiple
528 pathways like the abscisic acid-dependent transcription of embryo-specific target genes [64]. They
529 participate in regulation of salt stress tolerance and apoptotic signaling transduction [38,39].
530 Furthermore, they function in development of cotyledons [40]. The 14-3-3 υ isoform co-controls the
531 cell proliferation cycle and induces the division of chloroplasts, which results in an increased plastid
532 number, chlorophyll content and photosynthetic activity [40].
533   In this study, four 14-3-3 proteins could be identified to interact with PRX-IIE WT. 14-3-3
534 proteins are known to preferentially bind to phosphorylated motifs containing phosphoserine
535 residues [65,66]. In addition, pThr-dependent binding as well as non-phosphorylation dependent
536 interactions with target proteins were reported [67]. Phospho-mimetic variants of PRXIIE have been
537 used to further address the binding properties to 14-3-3 υ under defined redox-conditions. However,
538 preferential binding of 14-3-3 υ to these variants could not be detected under reducing as well as
539 oxidizing conditions. Instead, the highest binding could be observed for WT PRX-IIE under oxidizing
540 conditions (Figure 11B). In addition, introducing negative charges at positions S82, T108 and T223,
541 resulted in an inhibition of the thiol peroxidase activity (Figure 11A). Similar results have been
542 reported for human PRX2, where Cdk5-derived phosphorylation at T89 had a negative effect on its
543 activity [68].
544   To check, if the interaction of 14-3-3 υ and PRX-IIE under oxidizing conditions may alter the
545 peroxidase activity, the H_2O_2 reduction by PRX-IIE was determined using the FOX assay in the
546 presence or absence of 14-3-3υ (Figure 11C). A fivefold excess of 14-3-3 υ increased the peroxidase
547 activity of PRX-IIE significantly. Since such a high amount of 14-3-3 υ is necessary to alter the PRX-IIE
548 activity, it is more likely, that the interaction is important during signaling processes.

549 *4.6. Hypothetical outlook and where to go*

550   Several mechanistic scenarios may be hypothesized. Formation of regulatory assemblies of PRX-
551 IIE with homo- or heterodimers of 14-3-3 proteins may recruit additional binding partners. In such a
552 regulatory complex, proximity-based oxidation between oxidized PRX-IIE and reduced 14-3-3 υ or

553 the bound third partner could be the regulatory mechanism that leads to changes in function and
554 regulation of cellular processes (Figure **12**).
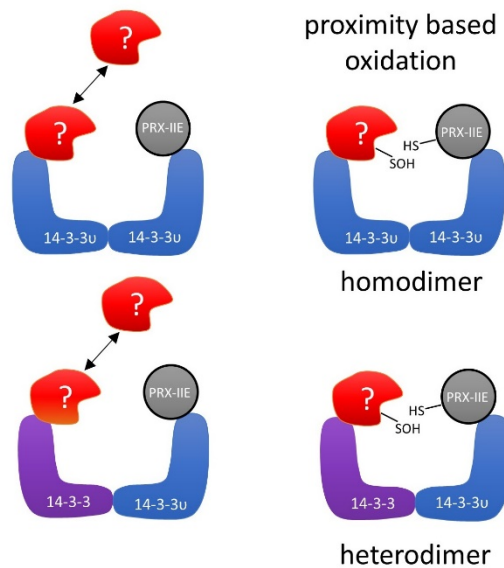
555

556 **Figure 12 Schematic depiction of the hypothetical interaction between PRX-IIE and 14-3-3 υ.**
557 Binding of oxidized PRX-IIE to 14-3-3 υ could induce association of a third partner. Formation of such
558 a complex could facilitate redox regulation, e.g. by proximity-based oxidation. The hypothetical
559 assembly may involve homo- or heterodimers of 14-3-3 isoforms.

560 As described previously, oxidative stress not just induces new interactions of 14-3-3 proteins
561 with protein partners, but also results in a loss of homeostatic interactions [69]. Under oxidative stress
562 in humans, the selenoprotein W binds to 14-3-3 with an intermolecular disulfide bridge. This process
563 results in a release of apoptosis signal-regulating kinase-1 (ASK1) from the 14-3-3-ASK1 complex.
564 ASK1 then activates the Jun N-terminal kinase and p38 MAP kinase pathways, which in turn activates
565 caspases and thereby apoptosis [69,70]. Therefore, PRX-IIE may affect several functions of 14-3-3 υ.
566 As indicated in figure 12, PRX-IIE could induce dimerization of 14-3-3 υ and, thereby, mediate the
567 binding or release of other proteins. Further studies are needed to address the importance of PRX-IIE
568 on 14-3-3 complex formation and their associated signaling pathways. It will also be important to
569 scrutinize the interaction of 14-3-3 proteins with the cytosolic PRX-IIB, C and D in the same functional
570 scenario of facilitating redox regulatory assemblies.

571

588
589   **Table S1 Primers used in this study for cloning.**

Gene	AGI	Restriction enzyme		Primer Sequence 5'->3'
GRX-S12	AT2G20270	NdeI	Forward	TTTCCAACATATGGGATCGACATTGGAGGAGACTG
		BamHI	Reverse	TTTCAGGATCCCTAGGTCTGACCGTTTTTTCC
SRX	AT1G31170	NdeI	Forward	ACATATGAACGGTTCGCCGCCGGTGAT
		BamHI	Reverse	AAAGGATCCTCAGCGAAGATGATGCCTTA
PRX-IIE	AT3G52960	NdeI	Forward	ATATACATATGGCCTCCATTTCCGTCGG
		BamHI	Reverse	ATATAGGATCCTCAGAGAGCTTTAAGCATATC
PRX-IIE C121S	AT3G52960		Forward	GGCGCATTCACACCAACAAGCTCAC
			Reverse	GTGAGCTTGTTGGTGTGAATG
PRX-IIE C146S	AT3G52960		Forward	AATCGCAAGTATCTCCGTCAAC
			Reverse	GACGGAGATACTTGCGATTACAT
PRX-IIE S82D	AT3G52960		Forward	GGTAGGAGAGAGTGTCGTCTGGGAGCTTGT
			Reverse	ACAAGCTCCCAGACGACACTCTCTCCTACC
PRX-IIE T108E	AT3G52960		Forward	GAACGGCGAATAGGATTTCTTTCTTCCCGGCG
			Reverse	CGCCGGGAAGAAAGAAATCCTATTCGCCGTTC
PRX-IIE T223E	AT3G52960		Forward	CTCAGCACTACTATTTTCAAAAGCACCTCCTTC
			Reverse	GAAGGAGGTGCTTTTGAAAATAGTAGTGCTGAG
PRX-IIE-EYFP	AT3G52960	BamHI	Forward	ATATAGGATCCATGGCGACTTCTCTCTCCGTTTC
		AgeI	Reverse	AAACCGGTGGGAGAGCTTTAAGCATATCCTCAG

590

Table S 2 Identified 14-3-3 proteins and their unique peptide.

Protein	AGI	Unique identified peptides	Identified peptides	Unique Peptide sequences	Localization	reference
14-3-3 χ	AT4G09000	11	25	DEFVYMAKLAEQAER DEFVYMAKLAEQAERYEEMVEFMEK DNLTLWTSDMQDDVADDIK DSTLIMQLLRDNLTLWTSDMQDDVADDIK DSTLIMQLLRDNLTLWTSDMQDDVADDIKEAAPAAAKPADEQQS EESRGNDDHVSLIRDYR GNDDHVSLIR GNDDHVSLIRDYR IETELSDICDGILK KDAAEHTLTAYK MATPGASSARDEFVYMAKLAEQAER	Cytosol, nucleus, chloroplast, golgi, vacuole	[71–75]
14-3-3 ω	AT1G78300	0	8		Cytosol, nucleus	[76]
14-3-3 φ	AT1G78300	4	14	DNLTLWTSDMQDESPEEIK EEFVYLAKLAEQAERYEEMVEFMEK GNDDHVTTIR LAEQAERYEEMVEFMEKVAEAVDK	Cytosol, nucleus, plasma membrane	[72,77,78]
14-3-3 υ	AT5G16050	8	17	ASWRIISSIEQKEDSR DNLTLWTSDLNDEAGDDIKEAPK DSTLIMQLLRDNLTLWTSDLNDEAGDDIK EDSRGNSDHVSIIK ICDGILNLLEAHLIPAASLAESK LGLALNFSVFYYEILNSSDR SAQDIALADLAPTHPIRLGLALNFSVFYYEILNSSDRACSLAK VDEQAQPPPSQ	Chloroplast, cytosol	[43]

Protein	AGI	Unique identified peptides	Identified peptides	Unique Peptide sequences	Localization	reference
14-3-3 λ	AT5G10450	5	7	DQYVYMAKLAEQAERYEEMVQFMEQLVTGATPAEELTVEER QAFEEAIAELDTLGEESYK QAFEEAIAELDTLGEESYKDSTLIMQLLR YEEMVQFMEQLVTGATPAEELTVEER YMAEFK	Nucleus, cytosol, plasma membrane, chloroplast	[79–81]
14-3-3 ν	AT3G02520	2	12	MSSSREENVYLAK TVDTDELTVEERNLLSVAYK	Chloroplast, Cytosol	[43]

592

593

594 References

595 1.   Horling, F.; Lamkemeyer, P.; König, J.; Finkemeier, I.; Kandlbinder, A.; Baier, M.; Dietz, K.-J. Divergent
596 light-, ascorbate-, and oxidative stress-dependent regulation of expression of the peroxiredoxin gene family in
597 Arabidopsis. *Plant Physiol.* **2003**, *131*, 317–325, doi:10.1104/pp.010017.

598 2.   Dietz,   K.-J.   Plant   peroxiredoxins.   *Annu.   Rev.   Plant   Biol.*   **2003**,   *54*,   93–107,
599 doi:10.1146/annurev.arplant.54.031902.134934.

600 3.   Dietz, K.-J.; Jacob, S.; Oelze, M.-L.; Laxa, M.; Tognetti, V.; Miranda, S.M.N. de; Baier, M.; Finkemeier, I. The
601 function of peroxiredoxins in plant organelle redox metabolism. *J. Exp. Bot.* **2006**, *57*, 1697–1709,
602 doi:10.1093/jxb/erj160.

603 4.   Brigelius-Flohé, R.; Flohé, L. Basic principles and emerging concepts in the redox control of transcription
604 factors. *Antioxid. Redox Signal.* **2011**, *15*, 2335–2381, doi:10.1089/ars.2010.3534.

605 5.   Baier, M.; Dietz, K.J. The plant 2-Cys peroxiredoxin BAS1 is a nuclear-encoded chloroplast protein: its
606 expressional regulation, phylogenetic origin, and implications for its specific physiological function in plants.
607 *Plant J.* **1997**, *12*, 179–190, doi:10.1046/j.1365-313x.1997.12010179.x.

608 6.   Collin, V.; Issakidis-Bourguet, E.; Marchand, C.; Hirasawa, M.; Lancelin, J.-M.; Knaff, D.B.; Miginiac-
609 Maslow, M. The Arabidopsis plastidial thioredoxins: new functions and new insights into specificity. *J. Biol.*
610 *Chem.* **2003**, *278*, 23747–23752, doi:10.1074/jbc.M302077200.

611 7.   Muthuramalingam, M.; Dietz, K.-J.; Ströher, E. Thiol‐Disulfide Redox Proteomics in Plant Research. In
612 *Plant Stress Tolerance: Methods and Protocols*; Sunkar, R., Ed.; Humana Press: Totowa, NJ, 2010; pp 219–238, ISBN
613 978-1-60761-702-0.

614 8.   Vaseghi, M.-J.; Chibani, K.; Telman, W.; Liebthal, M.F.; Gerken, M.; Schnitzer, H.; Mueller, S.M.; Dietz, K.-
615 J. The chloroplast 2-cysteine peroxiredoxin functions as thioredoxin oxidase in redox regulation of chloroplast
616 metabolism. *Elife* **2018**, *7*, doi:10.7554/eLife.38194.

617 9.   Lamkemeyer, P.; Laxa, M.; Collin, V.; Li, W.; Finkemeier, I.; Schöttler, M.A.; Holtkamp, V.; Tognetti, V.B.;
618 Issakidis-Bourguet, E.; Kandlbinder, A.; et al. Peroxiredoxin Q of Arabidopsis thaliana is attached to the
619 thylakoids and functions in context of photosynthesis. *Plant J.* **2006**, *45*, 968–981, doi:10.1111/j.1365-
620 313X.2006.02665.x.

621 10.   Romero-Puertas, M.C.; Laxa, M.; Mattè, A.; Zaninotto, F.; Finkemeier, I.; Jones, A.M.E.; Perazzolli, M.;
622 Vandelle, E.; Dietz, K.-J.; Delledonne, M. S-nitrosylation of peroxiredoxin II E promotes peroxynitrite-mediated
623 tyrosine nitration. *Plant Cell* **2007**, *19*, 4120–4130, doi:10.1105/tpc.107.055061.

624 11.   Rouhier, N.; Gelhaye, E.; Sautiere, P.E.; Brun, A.; Laurent, P.; Tagu, D.; Gerard, J.; Faÿ, E. de; Meyer, Y.;
625 Jacquot, J.P. Isolation and characterization of a new peroxiredoxin from poplar sieve tubes that uses either
626 glutaredoxin or thioredoxin as a proton donor. *Plant Physiol.* **2001**, *127*, 1299–1309.

627 12.   Stork, T.; Michel, K.-P.; Pistorius, E.K.; Dietz, K.-J. Bioinformatic analysis of the genomes of the
628 cyanobacteria Synechocystis sp. PCC 6803 and Synechococcus elongatus PCC 7942 for the presence of
629 peroxiredoxins and their transcript regulation under stress. *J. Exp. Bot.* **2005**, *56*, 3193–3206,
630 doi:10.1093/jxb/eri316.

631 13.   Declercq, J.P.; Evrard, C.; Clippe, A.; Stricht, D.V.; Bernard, A.; Knoops, B. Crystal structure of human
632 peroxiredoxin 5, a novel type of mammalian peroxiredoxin at 1.5 A resolution. *J. Mol. Biol.* **2001**, *311*, 751–759,
633 doi:10.1006/jmbi.2001.4853.

634 14.   Gama, F.; Bréhélin, C.; Gelhaye, E.; Meyer, Y.; Jacquot, J.-P.; Rey, P.; Rouhier, N. Functional analysis and
635 expression characteristics of chloroplastic Prx IIE. *Physiol Plant* **2008**, *133*, 599–610, doi:10.1111/j.1399-
636 3054.2008.01097.x.

637 15.   Horling, F.; König, J.; Dietz, K.-J. Type II peroxiredoxin C, a member of the peroxiredoxin family of
638 Arabidopsis thaliana: its expression and activity in comparison with other peroxiredoxins. *Plant Physiology and*
639 *Biochemistry* **2002**, *40*, 491–499, doi:10.1016/S0981-9428(02)01396-7.

640 16.   Couturier, J.; Ströher, E.; Albetel, A.-N.; Roret, T.; Muthuramalingam, M.; Tarrago, L.; Seidel, T.; Tsan, P.;
641 Jacquot, J.-P.; Johnson, M.K.; et al. Arabidopsis chloroplastic glutaredoxin C5 as a model to explore molecular
642 determinants for iron-sulfur cluster binding into glutaredoxins. *J. Biol. Chem.* **2011**, *286*, 27515–27527,
643 doi:10.1074/jbc.M111.228726.

644 17.   Ströher, E.; Dietz, K.-J. The dynamic thiol-disulphide redox proteome of the Arabidopsis thaliana
645 chloroplast as revealed by differential electrophoretic mobility. *Physiol Plant* **2008**, *133*, 566–583,
646 doi:10.1111/j.1399-3054.2008.01103.x.

18. König, J.; Baier, M.; Horling, F.; Kahmann, U.; Harris, G.; Schürmann, P.; Dietz, K.-J. The plant-specific function of 2-Cys peroxiredoxin-mediated detoxification of peroxides in the redox-hierarchy of photosynthetic electron flux. *Proc. Natl. Acad. Sci. U. S. A.* **2002**, *99*, 5738–5743, doi:10.1073/pnas.072644999.

19. Finkemeier, I.; Goodman, M.; Lamkemeyer, P.; Kandlbinder, A.; Sweetlove, L.J.; Dietz, K.-J. The mitochondrial type II peroxiredoxin F is essential for redox homeostasis and root growth of Arabidopsis thaliana under stress. *J. Biol. Chem.* **2005**, *280*, 12168–12180, doi:10.1074/jbc.M413189200.

20. Méchin, V.; Damerval, C.; Zivy, M. Total protein extraction with TCA-acetone. *Methods Mol. Biol.* **2007**, *355*, 1–8, doi:10.1385/1-59745-227-0:1.

21. Seidel, T.; Golldack, D.; Dietz, K.-J. Mapping of C-termini of V-ATPase subunits by in vivo-FRET measurements. *FEBS Letters* **2005**, *579*, 4374–4382, doi:10.1016/j.febslet.2005.06.077.

22. Seidel, T.; Kluge, C.; Hanitzsch, M.; Ross, J.; Sauer, M.; Dietz, K.-J.; Golldack, D. Colocalization and FRET-analysis of subunits c and a of the vacuolar H+-ATPase in living plant cells. *Journal of biotechnology* **2004**, *112*, 165–175, doi:10.1016/j.jbiotec.2004.04.027.

23. Muthuramalingam, M.; Matros, A.; Scheibe, R.; Mock, H.-P.; Dietz, K.-J. The hydrogen peroxide-sensitive proteome of the chloroplast in vitro and in vivo. *Frontiers in plant science* **2013**, *4*, 54, doi:10.3389/fpls.2013.00054.

24. Wessel, D.; Flügge, U.I. A method for the quantitative recovery of protein in dilute solution in the presence of detergents and lipids. *Anal. Biochem.* **1984**, *138*, 141–143, doi:10.1016/0003-2697(84)90782-6.

25. Jozefowicz, A.M.; Hartmann, A.; Matros, A.; Schum, A.; Mock, H.-P. Nitrogen Deficiency Induced Alterations in the Root Proteome of a Pair of Potato (Solanum tuberosum L.) Varieties Contrasting for their Response to Low N. *Proteomics* **2017**, *17*, doi:10.1002/pmic.201700231.

26. Arend, D.; Lange, M.; Chen, J.; Colmsee, C.; Flemming, S.; Hecht, D.; Scholz, U. e!DAL--a framework to store, share and publish research data. *BMC Bioinformatics* **2014**, *15*, 214, doi:10.1186/1471-2105-15-214.

27. Waterhouse, A.; Bertoni, M.; Bienert, S.; Studer, G.; Tauriello, G.; Gumienny, R.; Heer, F.T.; Beer, T.A.P. de; Rempfer, C.; Bordoli, L.; et al. SWISS-MODEL: homology modelling of protein structures and complexes. *Nucleic Acids Res.* **2018**, *46*, W296-W303, doi:10.1093/nar/gky427.

28. Schrödinger, L.L.C. *The PyMOL Molecular Graphics System, Version 2.4.0*, 2015.

29. Dietz, K.-J. Peroxiredoxins in plants and cyanobacteria. *Antioxid. Redox Signal.* **2011**, *15*, 1129–1159, doi:10.1089/ars.2010.3657.

30. Melchers, J.; Dirdjaja, N.; Ruppert, T.; Krauth-Siegel, R.L. Glutathionylation of trypanosomal thiol redox proteins. *J. Biol. Chem.* **2007**, *282*, 8678–8694, doi:10.1074/jbc.M608140200.

31. Park, J.W.; Piszczek, G.; Rhee, S.G.; Chock, P.B. Glutathionylation of peroxiredoxin I induces decamer to dimers dissociation with concomitant loss of chaperone activity. *Biochemistry* **2011**, *50*, 3204–3210, doi:10.1021/bi101373h.

32. Zaffagnini, M.; Bedhomme, M.; Marchand, C.H.; Morisse, S.; Trost, P.; Lemaire, S.D. Redox regulation in photosynthetic organisms: focus on glutathionylation. *Antioxid. Redox Signal.* **2012**, *16*, 567–586, doi:10.1089/ars.2011.4255.

33. Couturier, J.; Jacquot, J.-P.; Rouhier, N. Toward a refined classification of class I dithiol glutaredoxins from poplar: biochemical basis for the definition of two subclasses. *Frontiers in plant science* **2013**, *4*, 518, doi:10.3389/fpls.2013.00518.

34. Park, J.W.; Mieyal, J.J.; Rhee, S.G.; Chock, P.B. Deglutathionylation of 2-Cys peroxiredoxin is specifically catalyzed by sulfiredoxin. *J. Biol. Chem.* **2009**, *284*, 23364–23374, doi:10.1074/jbc.M109.021394.

35. Giustarini, D.; Rossi, R.; Milzani, A.; Colombo, R.; Dalle-Donne, I. S-glutathionylation: from redox regulation of protein functions to human diseases. *J. Cell. Mol. Med.* **2004**, *8*, 201–212, doi:10.1111/j.1582-4934.2004.tb00275.x.

36. Popov, D. Protein S-glutathionylation: from current basics to targeted modifications. *Archives of Physiology and Biochemistry* **2014**, *120*, 123–130, doi:10.3109/13813455.2014.944544.

37. Gasteiger, E.; Hoogland, C.; Gattiker, A.; Duvaud, S.'e; Wilkins, M.R.; Appel, R.D.; Bairoch, A. Protein Identification and Analysis Tools on the ExPASy Server. In *The Proteomics Protocols Handbook*; Walker, J.M., Ed.; Humana Press: Totowa, NJ, 2005; pp 571–607, ISBN 978-1-59259-890-8.

38. Ferl, R.J.; Manak, M.S.; Reyes, M.F. The 14-3-3s. *Genome Biol.* **2002**, *3*, REVIEWS3010, doi:10.1186/gb-2002-3-7-reviews3010.

39. Zhou, H.; Lin, H.; Chen, S.; Becker, K.; Yang, Y.; Zhao, J.; Kudla, J.; Schumaker, K.S.; Guo, Y. Inhibition of the Arabidopsis salt overly sensitive pathway by 14-3-3 proteins. *Plant Cell* **2014**, *26*, 1166–1182, doi:10.1105/tpc.113.117069.

40.   Vercruyssen, L.; Tognetti, V.B.; Gonzalez, N.; van Dingenen, J.; Milde, L. de; Bielach, A.; Rycke, R. de; van Breusegem, F.; Inzé, D. GROWTH REGULATING FACTOR5 stimulates Arabidopsis chloroplast division, photosynthesis, and leaf longevity. *Plant Physiol.* **2015**, *167*, 817–832, doi:10.1104/pp.114.256180.

41.   Chevalier, D.; Morris, E.R.; Walker, J.C. 14-3-3 and FHA domains mediate phosphoprotein interactions. *Annu. Rev. Plant Biol.* **2009**, *60*, 67–91, doi:10.1146/annurev.arplant.59.032607.092844.

42.   Dougherty, M.K.; Morrison, D.K. Unlocking the code of 14-3-3. *J. Cell Sci.* **2004**, *117*, 1875–1884, doi:10.1242/jcs.01171.

43.   Sehnke, P.C.; Henry, R.; Cline, K.; Ferl, R.J. Interaction of a plant 14-3-3 protein with the signal peptide of a thylakoid-targeted chloroplast precursor protein and the presence of 14-3-3 isoforms in the chloroplast stroma. *Plant Physiol.* **2000**, *122*, 235–242, doi:10.1104/pp.122.1.235.

44.   Cao, A.; Jain, A.; Baldwin, J.C.; Raghothama, K.G. Phosphate differentially regulates 14-3-3 family members and GRF9 plays a role in Pi-starvation induced responses. *Planta* **2007**, *226*, 1219–1230, doi:10.1007/s00425-007-0569-0.

45.   Aryal, U.K.; Krochko, J.E.; Ross, A.R.S. Identification of phosphoproteins in Arabidopsis thaliana leaves using polyethylene glycol fractionation, immobilized metal-ion affinity chromatography, two-dimensional gel electrophoresis and mass spectrometry. *J. Proteome Res.* **2012**, *11*, 425–437, doi:10.1021/pr200917t.

46.   Trujillo, M.; Clippe, A.; Manta, B.; Ferrer-Sueta, G.; Smeets, A.; Declercq, J.-P.; Knoops, B.; Radi, R. Pre-steady state kinetic characterization of human peroxiredoxin 5: taking advantage of Trp84 fluorescence increase upon oxidation. *Archives of Biochemistry and Biophysics* **2007**, *467*, 95–106, doi:10.1016/j.abb.2007.08.008.

47.   König, J.; Galliardt, H.; Jütte, P.; Schäper, S.; Dittmann, L.; Dietz, K.-J. The conformational bases for the two functionalities of 2-cysteine peroxiredoxins as peroxidase and chaperone. *J. Exp. Bot.* **2013**, *64*, 3483–3497.

48.   Sobotta, M.C.; Liou, W.; Stöcker, S.; Talwar, D.; Oehler, M.; Ruppert, T.; Scharf, A.N.D.; Dick, T.P. Peroxiredoxin-2 and STAT3 form a redox relay for H2O2 signaling. *Nat. Chem. Biol.* **2015**, *11*, 64–70, doi:10.1038/nchembio.1695.

49.   Liebthal, M.; Maynard, D.; Dietz, K.-J. Peroxiredoxins and Redox Signaling in Plants. *Antioxid. Redox Signal.* **2018**, *28*, 609–624.

50.   Barranco-Medina, S.; Krell, T.; Bernier-Villamor, L.; Sevilla, F.; Lázaro, J.-J.; Dietz, K.-J. Hexameric oligomerization of mitochondrial peroxiredoxin PrxIIF and formation of an ultrahigh affinity complex with its electron donor thioredoxin Trx-o. *J. Exp. Bot.* **2008**, *59*, 3259–3269.

51.   Sparla, F.; Fermani, S.; Falini, G.; Zaffagnini, M.; Ripamonti, A.; Sabatino, P.; Pupillo, P.; Trost, P. Coenzyme site-directed mutants of photosynthetic A4-GAPDH show selectively reduced NADPH-dependent catalysis, similar to regulatory AB-GAPDH inhibited by oxidized thioredoxin. *J. Mol. Biol.* **2004**, *340*, 1025–1037, doi:10.1016/j.jmb.2004.06.005.

52.   Bedhomme, M.; Zaffagnini, M.; Marchand, C.H.; Gao, X.-H.; Moslonka-Lefebvre, M.; Michelet, L.; Decottignies, P.; Lemaire, S.D. Regulation by glutathionylation of isocitrate lyase from Chlamydomonas reinhardtii. *J. Biol. Chem.* **2009**, *284*, 36282–36291, doi:10.1074/jbc.M109.064428.

53.   Rouhier, N.; Lemaire, S.D.; Jacquot, J.-P. The role of glutathione in photosynthetic organisms: emerging functions for glutaredoxins and glutathionylation. *Annu. Rev. Plant Biol.* **2008**, *59*, 143–166, doi:10.1146/annurev.arplant.59.032607.092811.

54.   Michelet, L.; Zaffagnini, M.; Marchand, C.; Collin, V.; Decottignies, P.; Tsan, P.; Lancelin, J.-M.; Trost, P.; Miginiac-Maslow, M.; Noctor, G.; et al. Glutathionylation of chloroplast thioredoxin f is a redox signaling mechanism in plants. *Proc. Natl. Acad. Sci. U. S. A.* **2005**, *102*, 16478–16483, doi:10.1073/pnas.0507498102.

55.   Park, S.-W.; Li, W.; Viehhauser, A.; He, B.; Kim, S.; Nilsson, A.K.; Andersson, M.X.; Kittle, J.D.; Ambavaram, M.M.R.; Luan, S.; et al. Cyclophilin 20-3 relays a 12-oxo-phytodienoic acid signal during stress responsive regulation of cellular redox homeostasis. *Proc. Natl. Acad. Sci. U. S. A.* **2013**, *110*, 9559–9564, doi:10.1073/pnas.1218872110.

56.   Hartmann, T.N.; Fricker, M.D.; Rennenberg, H.; Meyer, A.J. Cell-specific measurement of cytosolic glutathione in poplar leaves. *Plant Cell Environ.* **2003**, *26*, 965–975, doi:10.1046/j.1365-3040.2003.01031.x.

57.   Meyer, A.J.; Brach, T.; Marty, L.; Kreye, S.; Rouhier, N.; Jacquot, J.-P.; Hell, R. Redox-sensitive GFP in Arabidopsis thaliana is a quantitative biosensor for the redox potential of the cellular glutathione redox buffer. *Plant J.* **2007**, *52*, 973–986, doi:10.1111/j.1365-313X.2007.03280.x.

58.   König, K.; Vaseghi, M.J.; Dreyer, A.; Dietz, K.-J. The significance of glutathione and ascorbate in modulating the retrograde high light response in Arabidopsis thaliana leaves. *Physiol Plant* **2018**, *162*, 262–273, doi:10.1111/ppl.12644.

59. Kumar, V.; Vogelsang, L.; Seidel, T.; Schmidt, R.; Weber, M.; Reichelt, M.; Meyer, A.; Clemens, S.; Sharma, S.S.; Dietz, K.-J. Interference between arsenic-induced toxicity and hypoxia. *Plant Cell Environ.* **2019**, *42*, 574–590, doi:10.1111/pce.13441.

60. Chae, H.Z.; Oubrahim, H.; Park, J.W.; Rhee, S.G.; Chock, P.B. Protein glutathionylation in the regulation of peroxiredoxins: a family of thiol-specific peroxidases that function as antioxidants, molecular chaperones, and signal modulators. *Antioxid. Redox Signal.* **2012**, *16*, 506–523, doi:10.1089/ars.2011.4260.

61. Buchanan, B.B.; Balmer, Y. Redox regulation: a broadening horizon. *Annu. Rev. Plant Biol.* **2005**, *56*, 187–220, doi:10.1146/annurev.arplant.56.032604.144246.

62. Dreyer, A.; Schackmann, A.; Kriznik, A.; Chibani, K.; Wesemann, C.; Vogelsang, L.; Beyer, A.; Dietz, K.-J. Thiol Redox Regulation of Plant β-Carbonic Anhydrase. *Biomolecules* **2020**, *10*, doi:10.3390/biom10081125.

63. Jones, D.H.; Ley, S.; Aitken, A. Isoforms of 14-3-3 protein can form homo- and heterodimers in vivo and in vitro: implications for function as adapter proteins. *FEBS Letters* **1995**, *368*, 55–58, doi:10.1016/0014-5793(95)00598-4.

64. Schultz, T.F.; Medina, J.; Hill, A.; Quatrano, R.S. 14-3-3 proteins are part of an abscisic acid-VIVIPAROUS1 (VP1) response complex in the Em promoter and interact with VP1 and EmBP1. *Plant Cell* **1998**, *10*, 837–847, doi:10.1105/tpc.10.5.837.

65. Chung, H. The 14-3-3 proteins: cellular regulators of plant metabolism. *Trends in Plant Science* **1999**, *4*, 367–371, doi:10.1016/S1360-1385(99)01462-4.

66. Liang, X.; Da Paula, A.C.; Bozóky, Z.; Zhang, H.; Bertrand, C.A.; Peters, K.W.; Forman-Kay, J.D.; Frizzell, R.A. Phosphorylation-dependent 14-3-3 protein interactions regulate CFTR biogenesis. *Mol. Biol. Cell* **2012**, *23*, 996–1009, doi:10.1091/mbc.E11-08-0662.

67. van Heusden, G.P.H. 14-3-3 proteins: regulators of numerous eukaryotic proteins. *IUBMB Life* **2005**, *57*, 623–629.

68. Qu, D.; Rashidian, J.; Mount, M.P.; Aleyasin, H.; Parsanejad, M.; Lira, A.; Haque, E.; Zhang, Y.; Callaghan, S.; Daigle, M.; et al. Role of Cdk5-mediated phosphorylation of Prx2 in MPTP toxicity and Parkinson's disease. *Neuron* **2007**, *55*, 37–52, doi:10.1016/j.neuron.2007.05.033.

69. Pennington, K.L.; Chan, T.Y.; Torres, M.P.; Andersen, J.L. The dynamic and stress-adaptive signaling hub of 14-3-3: emerging mechanisms of regulation and context-dependent protein-protein interactions. *Oncogene* **2018**, *37*, 5587–5604, doi:10.1038/s41388-018-0348-3.

70. Ichijo, H.; Nishida, E.; Irie, K.; Dijke, P. ten; Saitoh, M.; Moriguchi, T.; Takagi, M.; Matsumoto, K.; Miyazono, K.; Gotoh, Y. Induction of apoptosis by ASK1, a mammalian MAPKKK that activates SAPK/JNK and p38 signaling pathways. *Science* **1997**, *275*, 90–94, doi:10.1126/science.275.5296.90.

71. Bae, M.S.; Cho, E.J.; Choi, E.-Y.; Park, O.K. Analysis of the Arabidopsis nuclear proteome and its response to cold stress. *Plant J.* **2003**, *36*, 652–663, doi:10.1046/j.1365-313x.2003.01907.x.

72. Ito, J.; Batth, T.S.; Petzold, C.J.; Redding-Johanson, A.M.; Mukhopadhyay, A.; Verboom, R.; Meyer, E.H.; Millar, A.H.; Heazlewood, J.L. Analysis of the Arabidopsis cytosolic proteome highlights subcellular partitioning of central plant metabolism. *J. Proteome Res.* **2011**, *10*, 1571–1582, doi:10.1021/pr1009433.

73. Helm, S.; Dobritzsch, D.; Rödiger, A.; Agne, B.; Baginsky, S. Protein identification and quantification by data-independent acquisition and multi-parallel collision-induced dissociation mass spectrometry (MS(E)) in the chloroplast stroma proteome. *J. Proteomics* **2014**, *98*, 79–89, doi:10.1016/j.jprot.2013.12.007.

74. Heard, W.; Sklenář, J.; Tomé, D.F.A.; Robatzek, S.; Jones, A.M.E. Identification of Regulatory and Cargo Proteins of Endosomal and Secretory Pathways in Arabidopsis thaliana by Proteomic Dissection. *Mol. Cell. Proteomics* **2015**, *14*, 1796–1813, doi:10.1074/mcp.M115.050286.

75. Yoshida, K.; Ohnishi, M.; Fukao, Y.; Okazaki, Y.; Fujiwara, M.; Song, C.; Nakanishi, Y.; Saito, K.; Shimmen, T.; Suzaki, T.; et al. Studies on vacuolar membrane microdomains isolated from Arabidopsis suspension-cultured cells: local distribution of vacuolar membrane proteins. *Plant Cell Physiol.* **2013**, *54*, 1571–1584, doi:10.1093/pcp/pct107.

76. Fakih, Z.; Ahmed, M.B.; Letanneur, C.; Germain, H. An unbiased nuclear proteomics approach reveals novel nuclear protein components that participates in MAMP-triggered immunity. *Plant Signal. Behav.* **2016**, *11*, e1183087, doi:10.1080/15592324.2016.1183087.

77. Mitra, S.K.; Walters, B.T.; Clouse, S.D.; Goshe, M.B. An efficient organic solvent based extraction method for the proteomic analysis of Arabidopsis plasma membranes. *J. Proteome Res.* **2009**, *8*, 2752–2767, doi:10.1021/pr801044y.

808   78.   Iglesias, J.; Trigueros, M.; Rojas-Triana, M.; Fernández, M.; Albar, J.P.; Bustos, R.; Paz-Ares, J.; Rubio, V.
809   Proteomics identifies ubiquitin-proteasome targets and new roles for chromatin-remodeling in the Arabidopsis
810   response to phosphate starvation. *J. Proteomics* **2013**, *94*, 1–22, doi:10.1016/j.jprot.2013.08.015.
811   79.   Rienties, I.M.; Vink, J.; Borst, J.W.; Russinova, E.; Vries, S.C. de. The Arabidopsis SERK1 protein interacts
812   with the AAA-ATPase AtCDC48, the 14-3-3 protein GF14lambda and the PP2C phosphatase KAPP. *Planta* **2005**,
813   *221*, 394–405, doi:10.1007/s00425-004-1447-7.
814   80.   Yasuda, S.; Sato, T.; Maekawa, S.; Aoyama, S.; Fukao, Y.; Yamaguchi, J. Phosphorylation of Arabidopsis
815   ubiquitin ligase ATL31 is critical for plant carbon/nitrogen nutrient balance response and controls the stability
816   of 14-3-3 proteins. *J. Biol. Chem.* **2014**, *289*, 15179–15193, doi:10.1074/jbc.M113.533133.
817   81.   Ferro, M.; Brugière, S.; Salvi, D.; Seigneurin-Berny, D.; Court, M.; Moyet, L.; Ramus, C.; Miras, S.; Mellal,
818   M.; Le Gall, S.; et al. AT_CHLORO, a comprehensive chloroplast proteome database with subplastidial
819   localization and curated information on envelope proteins. *Mol. Cell. Proteomics* **2010**, *9*, 1063–1084,
820   doi:10.1074/mcp.M900325-MCP200.